JOURNAL OF MATERIALS SCIENCE **38** (2003) 3535–3543

The load transfer effect in the true threshold creep behaviour of an Al-8.5Fe-1.3V-1.7Si alloy reinforced with alumina short fibres

K. KUCHAŘOVÁ, J. ČADEK
Institute of Physics of Materials, Academy of Sciences of the Czech Republic, 616 62 Brno, Czech Republic

S. J. ZHU
Institute of Industrial Science, The University of Tokyo, Tokyo 153 8505, Japan

The creep in an Al-8.5Fe-1.3V-1.7Si alloy dispersion strengthened with fine $Al_{12}(Fe,V)_3Si$ phase particles and reinforced with alumina short fibres—Composite in the following—is investigated at temperatures 648, 698 and 748 K. The results are compared with those obtained for the composite matrix Al-8.5Fe-1.3V-1.7Si alloy (Alloy in the following) at the same temperatures. Both, the Alloy and the Composite exhibit true threshold creep behaviour; the true threshold stress decreases rather strongly with increasing temperature. However, independently of temperature, it is about twice as high in the Composite than in the Alloy. This is explained employing the concept of the load transfer effect in the true threshold creep behaviour. The results strongly suggest that rather dramatic enhancement of creep resistance of an Al-8.5Fe-1.3V-1.7Si alloy can be reached introducing into it mechanically strong short fibres of micrometer dimensions, provided the aspect ratio of the fibres and their volume fraction are large enough.

1. Introduction

The Al-8.5Fe-1.3V-1.7Si (8009Al type) alloy processed by rapid solidification and powder metallurgy route is known to exhibit remarkable creep resistance up to temperature close to 750 K. This resistance is due to the high volume fraction (∼0.27) of fine (less than 50 nm in diameter) incoherent particles of the $Al_{12}(Fe,V)_3Si$ phase and relatively low coarsening rate of these particles at the temperatures mentioned above [1–6].

The Young's modulus of an aluminium alloy can be significantly enhanced by discontinuous reinforcement with hard unshearable ceramic particulates, short fibres or whiskers of micrometer dimensions even at temperatures as high as 700 K [7]. This fact motivated Peng *et al.* [8] and Zhu *et al.* [9] to reinforce an Al-8.5Fe-1.3V-1.7Si alloy with nitride whiskers and silicon carbide whiskers, respectively, as well as Ma and Tjong [5] and Čadek *et al.* [10, 11] with silicon carbide particulates. Beside increasing the Young's modulus, the discontinuous reinforcement can be expected to introduce the load transfer effect (e.g., [12–17]), under certain conditions at least [18]. Thus, while Peng *et al.* [8] and Zhu *et al.* [9] reported the load transfer effect in creep behaviour of an Al-8.5Fe-1.3V-1.7Si alloy reinforced with silicon nitride (Si_3N_4) or silicon carbide (SiC) whiskers, the load transfer effect was not detected by Ma and Tjong [5] investigated the creep behaviour of the alloy under consideration reinforced with 15 vol% SiC particulates at temperature 723 to 823 K. Moreover, Peng *et al.* [8] and Zhu *et al.* [9] found higher true threshold stress in the reinforced than in the unreinforced alloy. Later, also the present authors [6] reported significantly higher true threshold stress in the Al-8.5Fe-1.3V-1.7Si alloy reinforced with 15 vol% SiC particulates than in the unreinforced alloy. Since the discontinuous reinforcement such as particulates or whiskers do not represent effective obstacles to dislocations motion, the observed effect of enhanced true threshold stress as observed by the present authors [10] was suggested to follow from fine alumina particles appearing as a result of repeated atomisation of the alloy before reinforced alloy fabrication [10]. However, this suggestion had to be abandoned since a similar effect of reinforcement was observed in an ODS copper alloy reinforced with alumina short fibres [17].

In the ODS copper reinforced with 15 vol% alumina short fibres 3 μm in diameter and ∼19.5 μm in length the true threshold stress was approximately twice as high as that in the unreinforced ODS matrix alloy [17]. This dramatic increase of the true threshold stress was interpreted in terms of the factor by which the flow stress in the matrix is reduced due to load transfer and build-up of hydrostatic stresses (cf. [19]).

However, it should be pointed out that the load transfer may be partly or fully relaxed by diffusion assisted flow [18], i.e., by diffusion via reinforcement/matrix interfaces. Apparently, such a relaxation is more likely when the reinforcement is represented by particulates than when it is represented by short fibres aligned to

the direction of applied stress. This may explain some observations (e.g., [5]) of the absence of load transfer in alloys reinforced with mechanically strong particulates for which the aspect ratio is effectively close to 1. The investigation of ODS copper reinforced with alumina short fibres strongly suggests (cf. Fig. 9 in [17]) that the significantly higher creep strength of alumina short fibre reinforced ODS copper than that of unreinforced ODS copper is essentially due to the effect of the short fibre reinforcement on the true threshold stress.

Thus, taking into account the above results obtained investigating threshold creep behaviour of ODS copper and ODS copper reinforced with alumina short fibres it can be reasonably expected that the creep strength of an Al-8.5Fe-1.3V-1.7Si alloy can be rather dramatically increased by reinforcing it with ceramic short fibres of micrometer dimensions and the fibre aspect ratio (the length to the diameter of a fibre) at least ∼10 although also the dimensions of a fibre can play a significant role.

Therefore, the aim of the present investigation is to obtain new $\dot{\varepsilon}_m(\sigma, T)$ creep data ($\dot{\varepsilon}_m$ is the minimum creep strain rate, σ is the applied stress and T is the testing temperature) for an Al-8.5Fe-1.3V-1.7Si alloy and the same alloy reinforced with 15 vol% alumina short fibres of proper both dimensions and aspect ratio, and compare the results of data analysis with the prediction of the idea on the role of load transfer in the threshold creep behaviour of the dispersion strengthened alloys. This idea was presented in two previous papers of the authors [16, 17] and is very briefly outlined again in Section 4.1.

2. Materials and experimental procedures

The Al-8.5Fe-1.3V-1.7Si (8009Al type) alloy was melted in an induction furnace and argon atomised to powder of about 25 μm in particle size. Part of the alloy powder was mixed with alumina short fibres nominally 3 μm in diameter and ∼40 μm in length. The mixture was consolidated at 823 K and extruded at the same temperature to bars 12 mm in diameter. Another part of the alloy powder was processed in the same way as the mixture of the alloy powder and the alumina short fibres.

The resulting mean grain diameter was found close to 1 μm in the unreinforced alloy as well as in the alloy, reinforced with alumina short fibres, i.e., the composite. The structure of as extruded composite was reasonably homogeneous, although the $Al_{12}(Fe,V)_3Si$ phase particles (also fine alumina particles were necessarily present as a result of atomisation) were arranged in rows parallel to the extrusion direction as it is, as a rule, the case of the Al-8.5Fe-1.3V-1.7Si alloy processed by rapid solidification and powder metallurgy route (cf. Fig. 1 in [6]). Detailed studies of structure in alloys of this type were performed by Peng *et al.* [2, 3] and especially, by Carreño and Ruano [4].

From the bars of the alloy as well as from the bars of the composite, specimens for tensile creep tests 4.0 mm in diameter and 25.0 mm in gauge length were machined. The constant tensile stress creep tests were performed at the temperatures of 648, 698 and 748 K in purified argon; the testing temperatures were controlled

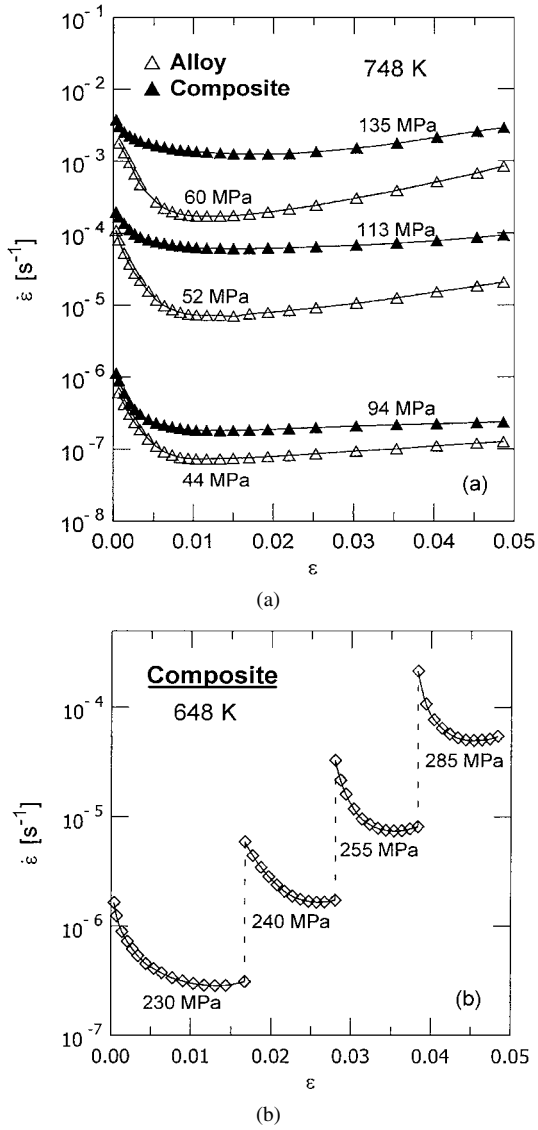

Figure 1 Representative examples of creep curves in the true creep strain rate $\dot{\varepsilon}$ versus true creep strain ε co-ordinates for the Alloy and the Composite at 748 K and various applied stresses (a). Examples of $\dot{\varepsilon}$ versus ε relations obtained using incremental applied stress creep test of the Composite at 648 K (b).

within 0.5 K. The creep elongation was measured by means of linear variable differential transducers coupled to a digital data acquisition system.

The technique of incremental stress creep tests was applied, although some tests at properly chosen stresses and various temperatures were performed running them well into tertiary creep stage if not to fracture to show that, as to the shape of creep curves, the Al-8.5Fe-1.3V-1.7Si alloy reinforced with alumina short fibres (the composite) exhibits the behaviour similar to that of the matrix alloy. This is illustrated in Fig. 1a. From the figure it can be seen that the steady state is not observed and that only the minimum creep strain rate $\dot{\varepsilon}_m$ can be defined at any testing temperature and applied stress.

Thus, an incremental isothermal creep stress change test was performed as follows (cf. [17, 20]). At a given applied stress σ, the creep strain rate $\dot{\varepsilon}$ was measured up to the creep strain, at which the creep strain rate started to increase indicating the onset of the tertiary creep stage at a given stress σ. Then, σ was increased by $\Delta\sigma$ to obtain the minimum creep strain rate at the

TABLE I Matrix Alloy and matrix Alloy - alumina - short - fibre Composite. Minimum creep strain rates $\dot{\varepsilon}_m$ measured at various testing temperatures T and various applied stresses σ

Alloy						Composite					
$T = 648$ K		$T = 698$ K		$T = 748$ K		$T = 648$ K		$T = 698$ K		$T = 748$ K	
σ (MPa)	$\dot{\varepsilon}_m$ (s^{-1})	σ (MPa)	$\dot{\varepsilon}_m$ (s^{-1})	σ (MPa)	$\dot{\varepsilon}_m$ (s^{-1})	σ (MPa)	$\dot{\varepsilon}_m$ (s^{-1})	σ (MPa)	$\dot{\varepsilon}_m$ (s^{-1})	σ (MPa)	$\dot{\varepsilon}_m$ (s^{-1})
162	1.1 E – 3	116	2.2 E – 3	75	5.1 E – 3	400	4.5 E – 3	270	6.0 E – 3	155	4.5 E – 3
151	4.7 E – 4	103	3.8 E – 4	60	1.8 E – 4	345	8.1 E – 4	235	1.8 E – 3	135	1.3 E – 3
137	1.1 E – 4	91	5.5 E – 5	60	3.5 E – 4	300	1.5 E – 4	210	2.7 E – 4	120	2.1 E – 4
131	4.6 E – 5	82	6.1 E – 6	56	5.5 E – 5	285	5.1 E – 5	183	3.5 E – 5	113	6.5 E – 5
115	2.9 E – 6	78	1.4 E – 6	52	7.5 E – 6	255	7.7 E – 6	167	5.4 E – 6	105	1.4 E – 5
109	5.7 E – 7	76	2.7 E – 7	46	7.0 E – 7	240	1.7 E – 6	163	1.4 E – 6	100	2.7 E – 6
106	8.1 E – 8	76	1.6 E – 7	44	7.8 E – 8	230	2.9 E – 7	160	4.1 E – 7	94	1.8 E – 7
103	7.8 E – 9	74	3.0 E – 8	43	8.5 E – 9	225	6.0 E – 8	155	4.6 E – 8	91	2.0 E – 8
101	1.9 E – 9	72	1.8 E – 9	42	1.4 E – 9	220	1.3 E – 8	153	6.5 E – 9	90	3.1 E – 9
						218	2.1 E – 9	152	1.2 E – 9	90	2.3 E – 9

stress $\sigma + \Delta\sigma$ and the above procedure was applied again (Fig. 1b). As a rule, two to five values of $\dot{\varepsilon}_m(\sigma)$ were obtained using one specimen.

3. Results

3.1. Al-8.5Fe-1.3V-1.7Si (matrix) alloy

The minimum creep strain rates $\dot{\varepsilon}_m$ in the Al-8.5Fe-1.3V-1.7Si alloy (simply Alloy in the following) measured at three temperatures T ranging from 648 to 748 K and various applied stresses σ are listed in Table I and plotted against σ in Fig. 2. It can be seen that the apparent stress exponent m_c of minimum creep strain rate defined as

$$m_c = \left(\frac{\partial \ln \dot{\varepsilon}_m}{\partial \ln \sigma}\right)_T \tag{1}$$

increases with decreasing applied stress at any temperature under consideration, which indicates the true threshold creep behaviour.

The true thershold stress is independent of applied stress by definition. At any given temperature it represents the stress bellow which the creep does not take place at all or, at least, does not take place by the same mechanism as above it. The true threshold stresses σ_{TH} at various temperatures were estimated using the linear extrapolation technique, e.g. [21, 22] based on plotting $\dot{\varepsilon}_m^{1/n}$ versus σ in double linear co-ordinates, where n is the true stress exponent. For the value of n characterising the operating creep strain rate controlling mechanism the relation between $\dot{\varepsilon}_m^{1/n}$ and σ is linear for each temperature; by its extrapolation to $\dot{\varepsilon}_m = 0$ the value of σ_{TH} is obtained.

For the Alloy investigated, the linear $\dot{\varepsilon}_m^{1/n}$ versus σ relations were found for $n \cong 5$ in accordance with the other works (e.g. [5, 6, 10]). This is demonstrated in Fig. 3. Values of σ_{TH} are equal to 95.9, 68.3 and 40.8 MPa at 648, 698 and 748 K, respectively. The linear correlation coefficients are given in the caption to this figure. Note that the values of the linear correlation coefficients are large; thus the choice of the exponent n and the estimated values of σ_{TH} are reliable. Values of σ_{TH} as well as σ_{TH}/G are plotted against temperature in Fig. 4. As expected (cf. [6, 10]) the true threshold stress σ_{TH} decreases with increasing temperature more strongly than the shear modulus G for aluminium [23].

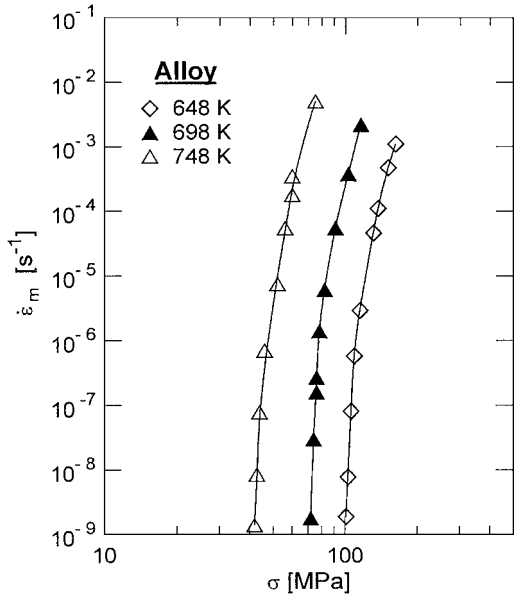

Figure 2 Alloy: relations between the measured minimum creep strain rate $\dot{\varepsilon}_m$ and applied stress σ at various testing temperatures.

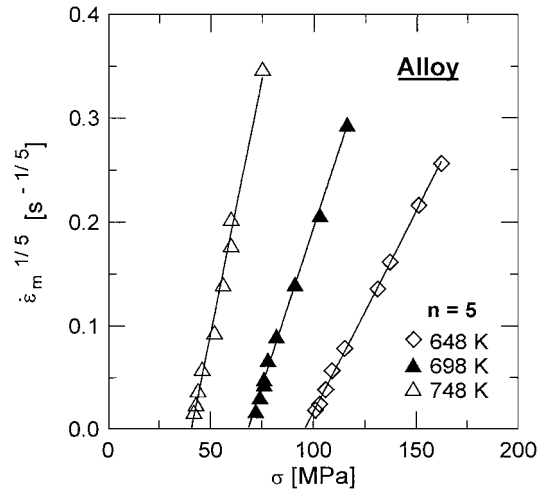

Figure 3 Alloy: relations between $\dot{\varepsilon}_m^{1/n}$ and σ at various temperatures for the true stress exponent $n = 5$. The true threshold stresses σ_{TH} are equal to 95.9, 68.3 and 40.8 at 648, 698 and 748 K, respectively. The linear correlation coefficient R_c ranges from 0.9994 to 0.9952.

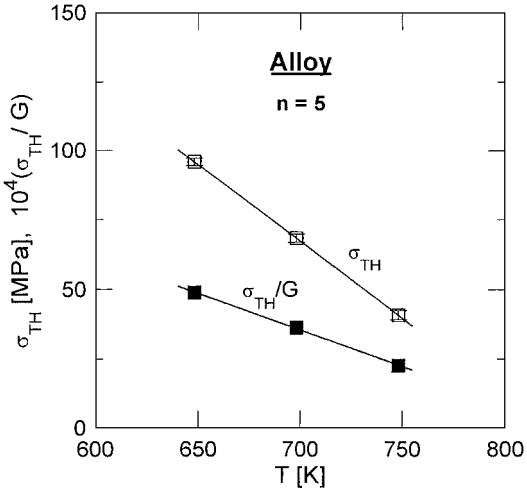

Figure 4 Alloy: relations between the true threshold stress σ_{TH} and temperature and between the true threshold stress to shear modulus ratio, σ_{TH}/G, and temperature. The derivative $d\sigma_{TH}/dT = -0.551$ MPa K^{-1}.

Referring to the several previous works (e.g. [6, 10]) it can be assumed that the creep strain rate in the alloy under consideration is lattice self-diffusion controlled. Therefore, in Fig. 5, the normalized minimum creep strain rates $\dot{\varepsilon}_m b^2/D_L$ are plotted against normalized effective stresses $(\sigma - \sigma_{TH})/G$; b is the length of the Burgers vector, D_L is the coefficient of lattice self-diffusion in aluminium [24]. It can be seen that all the data points can be well fitted by a single straight line in double logarithmic co-ordinates which strongly supports the above assumption that the creep strain rate is controlled by the lattice self-diffusion in the alloy matrix—aluminium. The slope of the line is close to the true stress exponent $n = 5$.

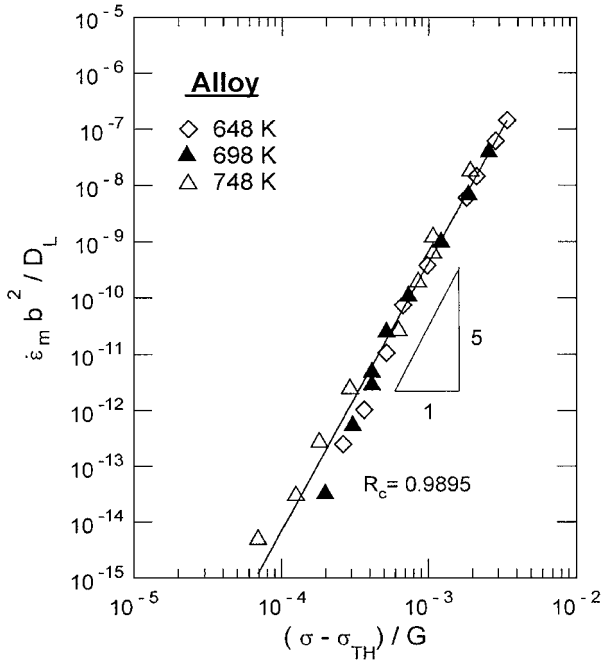

Figure 5 Alloy: the normalized minimum creep strain rate $\dot{\varepsilon}_m b^2/D_L$ plotted against normalized effective stress $(\sigma - \sigma_{TH})/G$. The values of D_L and G are those for the coefficient of lattice self-diffusion and for the shear modulus in pure aluminium, respectively.

3.2. Matrix alloy reinforced with alumina short fibres—the Composite

The minimum creep strain rates $\dot{\varepsilon}_m$ in the Composite measured at the temperatures of 648, 698 and 748 K and various applied stresses σ are listed in Table I and plotted against σ in double logarithmic co-ordinates in Fig. 6. It can be seen that, again, the apparent stress exponent m_c defined by Equation 1 increases with decreasing applied stress at any temperature under consideration, which indicates the true threshold creep behaviour. In this respect, the creep behaviour of the Composite is similar to that of its matrix Alloy.

The true threshold stresses σ_{TH} of the Composite were estimated by the same technique as those of the alloy. From Fig. 7, in which $\dot{\varepsilon}_m^{1/n}$ are plotted against σ in double linear co-ordinates it is apparent that the $\dot{\varepsilon}_m^{1/n}$ versus σ relations are linear for $n = 5$. Thus,

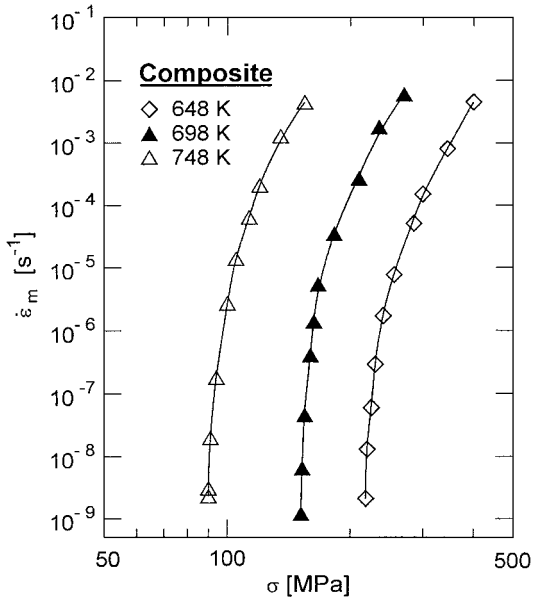

Figure 6 Composite: relations between the measured minimum creep strain rate $\dot{\varepsilon}_m$ and applied stress σ at various testing temperatures.

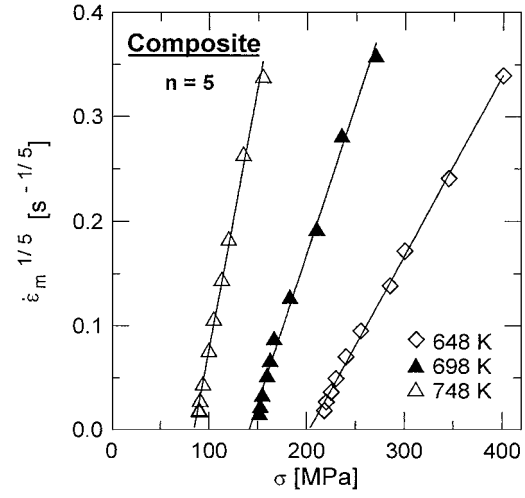

Figure 7 Composite: relations between $\dot{\varepsilon}_m^{1/n}$ and σ at various temperatures for $n = 5$. The true threshold stresses σ_{TH} are equal to 203.0, 141.7 and 84.9 MPa at 648, 698 and 748 K, respectively. The linear correlation coefficient R_c ranges from 0.9991 to 0.9962.

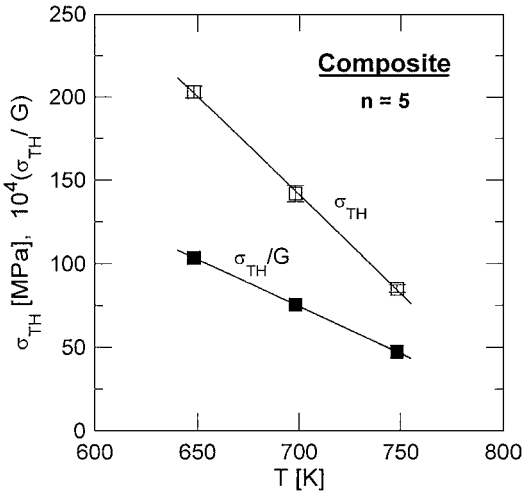

Figure 8 Composite: relations between the true threshold stress σ_{TH} and temperatures and between the true threshold stress to shear modulus ratio, σ_{TH}/G, and temperature. The derivative $d\sigma_{TH}/dT = -1.181$ MPa K^{-1}.

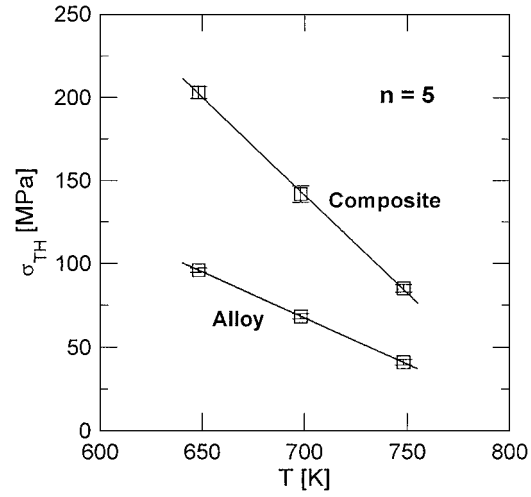

Figure 10 The true threshold stresses of the Composite as compared with those of the Alloy.

introducing the alumina short fibre reinforcement into the Alloy the true stress exponent n remains essentially unchanged. Values of σ_{TH} are equal to 203.0, 141.7 and 84.9 MPa at 648, 698 and 748 K, respectively. The linear correlation coefficients given in the caption to Fig. 7 are again large; thus the choice of the exponent n and the estimated values of σ_{TH} are fairly reliable. The values of σ_{TH} as well as the values of the σ_{TH}/G ratio are plotted against temperature in Fig. 8. The true threshold stress decreases with increasing temperature more strongly than the shear modulus G for aluminium.

Again, assuming that the minimum creep strain rate in the Composite is—similarly as in its matrix Alloy—controlled by the lattice self-diffusion in the latter, in Fig. 9 the normalized minimum creep strain rates $\dot{\varepsilon}_m b^2/D_L$ are plotted against normalized effective stresses $(\sigma - \sigma_{TH})/G$. All the data points can be fitted with a single straight line, which strongly supports the above assumption on the creep strain rate controlling process. The slope of the line in Fig. 9 is close to 5 and thus to the true stress exponent n.

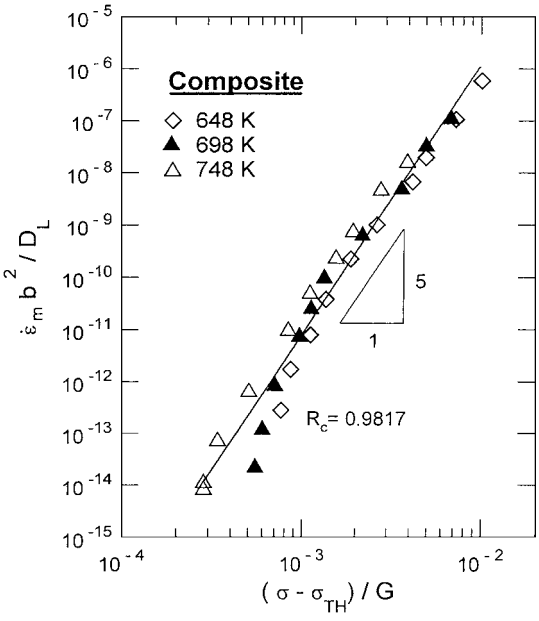

Figure 9 Composite: the normalized minimum creep strain rates $\dot{\varepsilon}_m b^2/D_L$ plotted against normalized effective stresses $\sigma_e/G = (\sigma - \sigma_{TH})/G$. The values of D_L and G are those for the coefficient of lattice self-diffusion in and the shear modulus of aluminium, respectively.

3.3. The true threshold stress of the Composite as compared with that of the Alloy

In Fig. 10, the relation between the true threshold stress and temperature for the Composite is compared with the similar relation for the Alloy. Both the relations are linear (cf. Figs 7 and 3). The ratios of σ_{TH} (C)/σ_{TH}(A) are equal to 2.11, 2.07 and 2.08 at the temperatures of 648, 698 and 748 K, respectively. Thus the σ_{TH}(C)/σ_{TH}(A) ratio is essentially temperature independent, its average value is equal to 2.09.

4. Discussion

4.1. The creep equation. Enhancement of the true threshold stress due to load transfer. The load transfer factor Λ

The minimum creep strain rate $\dot{\varepsilon}_m$ in the Alloy investigated displays the true threshold stress behaviour and thus can be described by the creep equation (cf. [6, 10])

$$\frac{\dot{\varepsilon}_m(A) b^2}{D_L} = A(A)\left(\frac{\sigma - \sigma_{TH}(A)}{G}\right)^n, \qquad (2)$$

where (A) denotes the alloy. A(A) is a dimensionless constant and σ_{TH}(A) is the true threshold stress of the alloy, which is independent of applied stress by definition.

Introducing a mechanically strong discontinuous reinforcement into the matrix, its creep strength is enhanced because the reinforcement impedes its plastic flow. The reinforcement strengthening can be

accounted for by a modified creep equation

$$\frac{\dot{\varepsilon}_m(C)b^2}{D_L} = A(A)\left(\frac{\sigma/\Lambda - \sigma_{TH}(A)}{G}\right)^n, \qquad (3)$$

where (C) denotes the composite exhibiting the dispersion and reinforcement strengthening and Λ is the factor, by which the flow stress of the Alloy is reduced due to load transfer and build-up of hydrostatic stresses. The factor Λ (the load transfer factor in the following) can be expressed as [19]

$$\Lambda \cong 1 + 2[2 + (l_R/d_R)]f_R^{\frac{3}{2}}, \qquad (4)$$

where l_R/d_R is the aspect ratio of the reinforcing short fibres (l_R is the length and d_R the diameter of a fibre) and f_R is the volume fraction of reinforcement. It should be pointed out that Equation 4 holds strictly for a stress exponent of the minimum creep strain rate approaching infinity ($m_c \to \infty$) and for short fibres aligned to the applied stress direction [19].

The creep Equation 3 can be rewritten as

$$\frac{\dot{\varepsilon}_m(C)b^2}{D_L} = A(C)\left(\frac{\sigma - \sigma_{TH}(C)}{G}\right)^n \qquad (5)$$

where

$$A(C) = A(A)/\Lambda^n \qquad (6)$$

and

$$\sigma_{TH}(C) = \Lambda\sigma_{TH}(A). \qquad (7)$$

Thus, the true threshold stress $\sigma_{TH}(C)$ of a dispersion and reinforcement strengthened metal (or solid solution alloy), i.e., the discontinuous composite with dispersion strengthened matrix is equal to the product $\Lambda\sigma_{TH}(A)$.

The above simple modelling illustrated in Fig. 1 in [17] is, in a way, similar to that performed recently by Rösler and Bäker [19] and illustrated in their Fig. 5. These authors accepted the creep model developed by Rösler and Arzt [25], which is based on thermally activated detachment of dislocations from interacting particles as the creep strain rate controlling mechanism. They do not admit the existence of the true threshold stress arguing that the energy necessary for thermally activated detachment of a dislocation from an interacting particle is low and thus always attainable in the detachment event.

However, the true threshold creep behaviour of the Alloy (and the same holds for the Composite) under consideration apparently represents a reality at least at temperatures ranging from 648 to 748 K, provided the apparent stress exponent m_c (Equation 1) increasing with decreasing applied stress is taken as the relevant criterion of such a behaviour. According to the above brief analysis, the true threshold creep behaviour of an Al-8.5Fe-1.3V-1.7Si alloy reinforced with alumina short fibres should be expected, since the matrix exhibits the behaviour in question.

4.2. The load transfer factor Λ and the true threshold stress

It is well known (e.g. [21, 22]) that mechanically strong particulates or short fibres of micrometer dimensions do not act as effective obstacles to moving dislocations. In fact, the Orowan bowing stress associated with such obstacles is very low even at volume fractions of particulates or short fibres as high as ~0.3. Thus, such reinforcement *in itself* cannot cause the threshold creep behaviour. The true threshold creep behaviour is always associated with the presence of mechanically strong particles of nanometer dimensions that are incoherent with the matrix. The true threshold stress in an Al-8.5Fe-1.3V-1.7Si alloy is due to the presence of fine $Al_{12}(Fe,V)_3Si$ phase particles. However, reinforcing this alloy with 15 vol% alumina short fibres of nominally 3 μm in diameter, the true treshold stress approximately twice as high is obtained. According to the idea outlined in Section 4.1 the reinforcement may enhance the true threshold stress of a dispersion strengthened alloy due to load transfer, i.e., due to impeding the plastic flow of the dispersion strengthened matrix of the Composite. This idea can be considered quite relevant.

According to Equation 7, the true threshold stress of the Composite is by a factor Λ higher than the true threshold stress of the (dispersion strengthened) Alloy. Provided the conditions of strict validity of Equation 4 are fulfilled, the factor Λ can be calculated by means of this equation. Of course, to apply Equation 4 the aspect ratio l_R/d_R of alumina short fibres must be known. In the present work, the average length of short fibres in the Composite could not be estimated by a technique of microstructural analysis. However, according to Equation 7, $\Lambda = \sigma_{TH}(C)/\sigma_{TH}(A)$: thus the factor Λ defined this way is denoted as the "effective" load transfer factor Λ^{exp} in the following. The factor Λ^{exp} is equal to 2.11, 2.07 and 2.08 at 648, 698 and 748 K, respectively (see Section 3.3). In average Λ^{exp} is equal to 2.09. Accepting this value of Λ, the "effective" aspect ratio l_R/d_R was estimated by means of Equation 4. Setting $\Lambda^{exp} = 2.09$ and $f_R = 0.15$, the "effective" aspect ratio equal to 7.4 is obtained. The length of alumina fibres (~3 μm in diameter) used to produce the composite was nominally ~40 μm (Section 2). However, many of the fibres, if not all, were broken during the composite processing. Hence, the above effective aspect ratio seems reasonable. From this aspect ratio, the average length of a fibre in the Composite is approximately equal to 22.2 μm.

The conditions of validity of Equation 4 may not be strictly fulfilled. This concerns especially alignment of the short fibres with the extrusion direction and thus with the applied stress direction. On the other hand, the conditions concerning the value of applied stress exponent is most probably fulfilled tolerably, since at the applied stresses only slightly higher than the true threshold stresses the apparent stress exponent m_c, (Equation 1), reaches very high values at each temperature under consideration (see Fig. 6). It should be expected that, introducing the reinforcement, the structure of the matrix Alloy is more or less

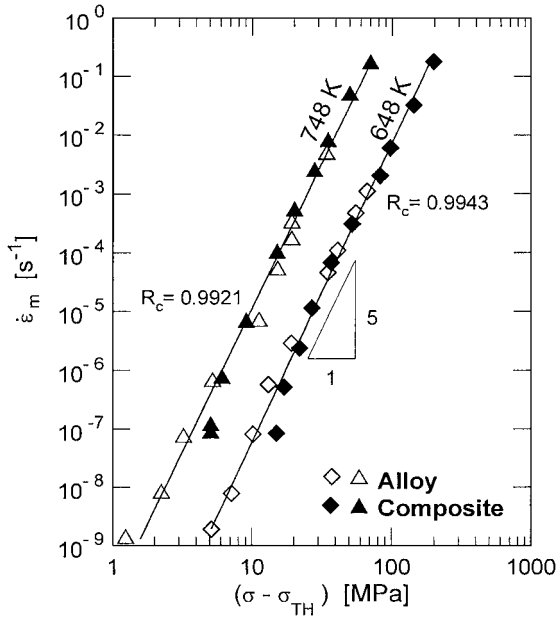

Figure 11 Relations between minimum creep strain rate $\dot{\varepsilon}_m$ and the effective stress $\sigma_e = \sigma - \sigma_{TH}$. The dimensionless constant $A = A(A)$ in the creep equation for the Alloy–Equation 2—was estimated from creep data to 3.299×10^{-10} and to 4.492×10^{-13} for 748 K and for 648 K, respectively. Values of the constant $A = A(C)$ in the creep equation for the Composite—Equation 5—were calculated using the relation $A(C) = A(A)/\Lambda^n$, Equation 6, setting 5 for n and 2.09 for Λ. The creep strain rates $\dot{\varepsilon}_m$ in the Composite were then calculated by means of Equation 5.

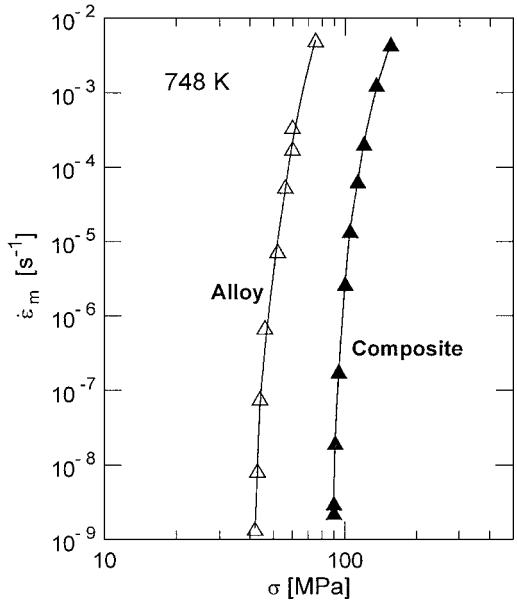

Figure 12 Effect of the short fibre reinforcement on the creep strength of the Alloy. Relations between the minimum creep strain rate $\dot{\varepsilon}_m$ and applied stress σ for the Composite at 748 K, compared with a similar relation for the Alloy.

modified, which might slightly affect the load transfer factor Λ^{exp}.

In Fig. 11, the minimum creep strain rates $\dot{\varepsilon}_m$ are plotted against effective stress $\sigma_e = \sigma - \sigma_{TH}$ for both the Alloy and the Composite at 648 and 748 K. The procedure used to obtain these $\dot{\varepsilon}_m$ vs. $(\sigma - \sigma_{TH})$ relations is described in caption to Fig. 11, from which it can be seen that $\dot{\varepsilon}_m$ vs. $(\sigma - \sigma_{TH})$ data plots for the alloy and the composite can be very well fitted by a single straight line for 648 K, that the same holds for 748 K and, finally, that the slopes of straight lines are very close to the true stress exponent n, i.e., to 5. The figure thus strongly supports the above conclusion that the effective load transfer factor Λ^{exp} is in average equal to 2.09.

4.3. Applied stress and temperature dependence of the apparent activation energy Q_c^{corr} and of the apparent stress exponent m_c

In a concurrent paper [26] it is shown that the apparent activation energy of creep corrected for the temperature dependence of shear modulus, Q_c^{corr}, in both the Alloy and the Composite decreases with increasing applied stress as well as with increasing temperature. At the applied stresses only slightly higher than the true threshold stress it reaches values many times higher than the true activation energy of creep, i.e., the activation enthalpy of lattice self-diffusion in aluminium $\Delta H_L = 142$ kJ mol^{-1} [24]. These differences are fully explained in terms of the temperature dependence of the true threshold stress (cf. [17, 20]). Also, it is shown that the apparent stress exponent m_c of the minimum creep strain rate in creep of both the Alloy and the Composite is generally higher (or even much higher) than the true stress exponent n. The applied stress dependence of the exponent m_c is inherent to the true threshold creep behaviour. Its temperature dependence follows from the temperature dependence of the true threshold stress (cf. [17, 20]).

4.4. Effect of the short fibre reinforcement on the strength of the alloy

In Fig. 12, the relation between minimum creep strain rate $\dot{\varepsilon}_m$ and applied stress σ for the Composite at 748 K is compared with a similar relation for the Alloy. At the lowest applied stress at which the minimum creep strain rate was measured in the Composite, i.e., at 90 MPa, the creep strain rate of the Alloy is by ~7 orders of magnitude higher than that in the Composite. Thus, the creep strengthening of the alumina short fibre reinforced Alloy is dramatic. Comparing visually the relations between $\dot{\varepsilon}_m$ and σ for the Composite and the Alloy one can conclude that the strengthening effect of the short fibre reinforcement is almost exclusively due to its effect on the true threshold stress. This is in agreement with the analysis of the $\dot{\varepsilon}_m(\sigma, T)$ data presented above.

5. Additional remarks

5.1. Temperature dependence of the true threshold stress

Although the true threshold stress in the Composite is by a factor ~2 higher than that in the unreinforced Alloy, its origin is the same as in the latter. The true threshold stress σ_{TH} is supposed to originate from an attractive interaction of dislocations with fine incoherent $Al_{12}(Fe,V)_3Si$ phase particles [10]. As suggested

[6, 10], it can be identified with the athermal detachment stress σ_d, expressed as

$$\sigma_d = \sigma_{OB}\sqrt{1 - k_R^2}, \quad (8)$$

where σ_{OB} is the Orowan bowing stress and k_R is the relaxation factor [27, 28]. However, such an identification of σ_{TH} with σ_d is possible only if the relaxation factor k_R is admitted to increase with increasing temperature, since the Orowan bowing stress is proportional to the shear modulus [29] and the true threshold stress decreases with increasing temperature more strongly than this modulus, Figs 4 and 8. Such an interpretation of the origin of the strong temperature dependence of the true threshold stress was suggested by the present authors [6, 10]. In a very recent paper, Spigarelli [30] has strongly supported this suggestion (see Fig. 14 in [30]).

5.2. Volume fraction of the "active" $Al_{12}(Fe,V)_3Si$ phase particles

The volume fraction of the $Al_{12}(Fe,V)_3Si$ phase particles in the Al-8.5Fe-1.3V-1.7Si type alloy is, as a rule, reported [1, 2, 4, 6] to be ~0.27. A careful analysis has led Spigarelli [30] to the conclusion that far from all dispersed $Al_{12}(Fe,V)_3Si$ particles act as obstacles to moving dislocations. In the Alloy, the volume fraction of "active" particles has been estimated to 0.04. In the Alloy reinforced with 15 vol% SiC particulates the volume fraction of active particles is slightly higher namely ~0.05. The difference between the total volume fraction and the volume fraction of active particles is explained by the particles being predominantly located at grain boundaries; of course, these particles cannot interact with lattice dislocations [30]. An introduction of the discontinuous reinforcement into the matrix alloy should be expected to modify the structure of the latter (see Section 4.2). This structure modification thus seems to be primarily manifested by the higher active particle volume fraction in the Alloy. But such a modification of the structure of the Composite cannot in itself fully explain the higher true threshold stresses in the Composite than in its matrix Alloy.

6. Summary and conclusions

Creep in an Al-8.5Fe-1.3V-1.7Si (8009Al type) alloy strengthened with $Al_{12}(Fe,V)_3Si$ phase particles of nanometer dimensions and the same Alloy reinforced with alumina short fibres of micrometer dimensions—the Composite—is investigated at temperatures 648, 698 and 748 K. The analysis of the creep data leads to the following main conclusions.

1. The minimum creep strain rate $\dot{\varepsilon}_m$ is apparently controlled by the lattice self-diffusion in the Alloy matrix—aluminium—and the true stress exponent n of minimum creep strain rate is very close to 5.

2. Both the Alloy and the Composite exhibit true threshold creep behaviour. The true threshold stress decreases with increasing temperature more strongly than the shear modulus in aluminium. However, it is about twice as high in the Composite than in the matrix Alloy. This is explained employing the concept of the load transfer effect in the true threshold creep behaviour, Section 4.1.

3. The results and their analysis strongly suggest that rather dramatic enhancement of creep resistance of an A1-8.5Fe-1.3V-1.7Si alloy can be reached introducing into it mechanically strong short fibres of micrometer dimensions. the volume fraction of the fibres must be large enough (e.g., 0.15) and the aspect ratio of short fibres must be high enough (e.g., 10). Also the dimensions of short fibres should be large enough to prevent load transfer relaxation by diffusional flow. Hence, the mean diameter of a short fibre should not be less than about 3 μm.

Acknowledgments

The present work was financially supported by the Grant Agency of the Academy of Sciences of the Czech Republic (Grant AV ČR No. S2041001). The authors thank Dr. Alena Orlová for comments on the manuscript and Ms. Eva Najvarová for assistance in manuscript preparation.

References

1. F. CARREÑO, G. GONZALES-DONCEL and O. A. RUANO, *Mater. Sci. Eng.* A **164** (1993) 216.
2. L. M. PENG, S. J. ZHU, Z. Y. MA, F. G. WANG and H. R. CHEN, *J. Mater. Sci.* **33** (1998) 5643.
3. L. M. PENG, S. J. ZHU, Z. Y. MA, J. BI, H. R. CHEN and F. G. WANG, *Mater. Sci. Eng.* A **259** (1998) 25.
4. F. CARREÑO and O. A. RUANO, *Acta Mater.* **46** (1998) 159.
5. Z. Y. MA and S. J. TJONG, *Mater. Sci. Eng.* A **278** (2000) 5.
6. S. J. ZHU, K. KUCHAŘOVÁ and J. ČADEK, *Metall. Mater. Trans.* A **31A** (2000) 2229.
7. D. J. LLOYD, *Int. Mater. Rev.* **39** (1994) 1.
8. L. M. PENG, S. J. ZHU, Z. Y. MA, J. BI, H. R. CHEN and F. G. WANG, *Comp. Sci. Tech.* **59** (1999) 769.
9. S. J. ZHU, L. M. PENG, Q. ZHOU, Z. Y. MA, J. BI, F. G. WANG and Z. G. WANG, *Mater. Sci. Eng.* A **215** (1996) 120.
10. J. ČADEK, K. KUCHAŘOVÁ and S. J. ZHU, *ibid.* A **283** (2000) 172.
11. *Idem.*, *ibid.* **297** (2001) 176.
12. A. KELLY and K. N. STREET, *Proc. Roy. Soc. London* A **328** (1573) (1972) 283.
13. K.-T. PARK and A. MOHAMED, *Metall. Mater. Trans.* A **26A** (1995) 3119.
14. Y. LI and T. G. LANGDON, *ibid.* **29A** (1998) 2523.
15. H. LI, J. B. LI, Z. Y. KONG and Z. G. WANG, *J. Mater. Sci. Lett.* **15** (1996) 616.
16. J. ČADEK and K. KUCHAŘOVÁ, *Kovove Mater.* **41** (2003) 127.
17. K. KUCHAŘOVÁ, S. J. ZHU and J. ČADEK, *Mater. Sci. Eng.* A **348** (2003) 170.
18. J. RÖSLER, G. BAO and A. G. EVANS, *Acta Metall. Mater.* **39** (1991) 616.
19. J. RÖSLER and M. BÄKER, *Acta Mater.* **48** (2000) 3553.
20. K. KUCHAŘOVÁ, S. J. ZHU and J. ČADEK, *Mater. Sci. Eng.* A, **355** (2003) 267.
21. R. LAGNEBORG and B. BERGMAN, *Met. Sci.* **10** (1976) 20.
22. J. ČADEK, H. OIKAWA and V. ŠUSTEK, *Mater. Sci. Eng.* A **190** (1995) 9.
23. J. E. BIRD, A. K. MUKHERJEE and J. E. DORN, in "Quantitative Relations Between Properties and Microstructure,"

edited by D. G. Brandon and A. Rosen (Israel University Press, Jerusalem 1969) p. 255.
24. T. S. LUNDY and J. F. MURDOCK, *J. Appl. Phys.* **33** (1972) 1671.
25. J. RÖSLER and E. ARZT, *Acta Metall. Mater.* **38** (1990) 671.
26. K. KUCHAŘOVÁ, S. J. ZHU and J. ČADEK, *Kovove Mater.* **40** (2002) 69.
27. E. ARZT and D. S. WILKINSON, *Acta Metall.* **34** (1986) 1893.
28. E. ARZT and J. RÖSLER, *ibid*. **36** (1988) 1053.
29. U. F. KOCKS, *Philos. Mag.* **13** (1966) 541.
30. S. SPIGARELLI, *Mater. Sci. Eng.* A **337** (2002) 306.

Received 4 March
and accepted 16 June 2003